A Localized Defect Detection of Rolling Element Bearing Using A New Indicator for Morlet Wavelet Filter Adjustment

Nuntaphong Koondilogpiboon[1] and Chairote Kunpanitchakit[*1]

1 Department of Mechanical Engineering, Faculty of Engineering, Chulalongkorn University, Bangkok, Thailand 10330

* Corresponding Author: Tel: 02 218 6632 E-mail: chairote.k@chula.ac.th

Abstract

Failures of rolling element bearing can cause serious downtime. Early stage bearing defects require a special detection method. When localized defect occurs, the periodic impulse which relates to bearing defect location appears in machinery vibration signal. High frequency resonance technique (HFRT) or envelope analysis is used in conjunction with complex Morlet wavelet because it resembles to mechanical impulse. This detection method demodulates defect-related low frequency part from system-natural-frequency-related high frequency part. However a proper indicator for optimal center frequency and bandwidth is needed to obtain promising detection result.

This study proposes an indicator that picks optimal Morlet wavelet that gives the highest ratio of the sum of harmonics family that has maximum value to the arithmetic mean of envelope spectrum in a specified range. In simulation study, it is shown that the proposed parameter can detect bearing defect not less than 97% from signal of various natural frequencies and damping ratios up to signal to noise ratio of -15 dB. The real bearing experiment was conducted with outer race defect under various defect sizes, radial loads and shaft speeds. It is shown that the indicator can successfully detect all cases of defect on outer race if line resolution in envelope spectrum is chosen properly.

Keywords*:* Rolling Element Bearing Defect Detection, Wavelet Filtering, Envelope Spectrum, Morlet Wavelet, Optimal Wavelet Indicator.

1. Introduction

Rolling element bearings are vital for rotating machinery. Bearing failures contribute major cause of machinery breakdown resulting in costly downtime. To prevent that, bearing condition monitoring methods have been developed. Vibration monitoring has been widely used since it reveals bearing failures more efficiently than other methods. [1]

Typical failure mode of rolling element bearings are usually caused by localized defect that occurs when a small piece of material is dislodged from bearing contact surface, mostly due to fatigue under cyclic contact stress [2]. When mating contact element runs pass this defect, wide band impulses are generated periodically at bearing defect characteristic

frequency. Hence, the vibration signal of defective bearings can be viewed as an impulse response of this impulse train. This amplitude modulated signal consists of defect characteristic frequency which acts as low frequency modulator and bearing-support system natural frequency as high frequency carrier [3, 4]. This frequency tells us which part of the bearing the defect is on. Unfortunately, the energy of this signal spreads across wide frequency range, and it is buried in noise or other unrelated signal, especially at low frequency where other mechanical vibrations dominate [5].

To overcome this problem, many methods have been developed. One of most widely recognized method is high frequency resonance technique (HFRT) or envelope analysis [1, 6] which is a combination of bandpass filtering, enveloping and spectrum construction. This method provides periodic excitation extraction and defective signal demodulation. However, this method requires selection of filter frequency band in order to obtain effective result [7].

Recently, wavelet-based filter have been applied in bearing fault detection in conjunction with HFRT due to its flexible time-frequency resolution and transient signal detection capability. Among many type of wavelets, Morlet wavelet is commonly used due to its impulse-like feature [3, 8, 9]. But, similar to ordinary bandpass filter, it also requires proper parameters (center frequency and bandwidth) in order to obtain good result. To achieve these optimal parameters, some indicators have been proposed such as Shannon entropy [3, 8] or kurtosis of envelope of filtered signal [9]. But both indicators do not take harmonic feature of envelope spectrum, which is strongly related to impulse train excited by localized defect, into account. Thus, this paper proposes a new indicator for Morlet wavelet parameter adjustment in envelope analysis that takes harmonics in envelope spectrum into account.

2. Review on signal processing

2.1 Wavelet transformation

The wavelet is obtained from a function $\psi(t)$ by translation and scaling [10] as:

$$\psi_{(a,\tau)}(t) = \frac{1}{\sqrt{a}}\psi\left(\frac{t-\tau}{a}\right) \quad (1)$$

Where a is scale and τ is translation and $\psi(t)$ is "mother wavelet". The wavelet transform of a finite energy signal $x(t)$ is the convolution of $x(t)$ with conjugate of Eq. (1) or "daughter" wavelet as:

$$WT(a,\tau) = \frac{1}{\sqrt{a}}\int_{-\infty}^{\infty} x(t)\frac{1}{\sqrt{a}}\psi^*\left(\frac{t-\tau}{a}\right)dt \quad (2)$$

Where $\psi^*(t)$ is complex conjugation of $\psi(t)$.

Since main interest in bearing defect detection is to extract impulse-like features in the signal, the Morlet wavelet is used due to it is more resemble to mechanical impulse than other mother wavelet [11]. The Morlet wavelet can be defined in time domain as complex sinusoidal enveloped by Gaussian function [9]

$$\psi(t) = \frac{\sigma}{\sqrt{\pi}}e^{-\sigma^2 t^2}e^{i2\pi f_0 t} \quad (3)$$

Where σ and f_0 are wavelet shape factor and center frequency, respectively.

The Fourier spectrum of Eq. (3) can be written as:

$$\Psi(f) = e^{-(\pi^2/\sigma^2)(f-f_0)^2} \quad (4)$$

Since wavelet transform can be written in form of Fourier transform [10], Eq. (2) can be written in frequency domain as:

$$WT(a,\tau) = \sqrt{a}\cdot IFT\{X(f)\Psi^*(af)\} \quad (5)$$

Where $X(f)$ and $\Psi(f)$ are Fourier spectrum of $x(t)$ and $\psi(t)$, respectively. And IFT denotes the inverse Fourier transform. Eq. (5) indicates that wavelet transform can be considered as filtering operation where $\psi(t)$ acts as filters that has center frequency at f_0 and its bandwidth is controlled by σ. Since definition of bandwidth is open, half power bandwidth is defined as:

$$\beta = \frac{\sqrt{2\ln 2}}{\pi}\sigma \qquad (6)$$

Eq. (6) dictates that power spectrum at the ends of the passband $\{f_0 - \beta/2,\ f_0 + \beta/2\}$, are half of its own maximum value. By substituting Eq. (6), Eq. (4) can be rewritten as:

$$\Psi(f) = e^{-(-2\ln 2/\beta^2)(f-f_0)^2} \qquad (7)$$

Hence, filtered signal from Morlet wavelet that has center frequency f_0 and bandwidth β can be obtained by using Eq. (5) and Eq. (7).

$$WT(f_0,\beta) = IFT\{X(f)\Psi^*(f)\} \qquad (8)$$

Note that Eq. (8) makes use of the inverse fast Fourier transform (IFFT) subroutine in MATLAB available. An example of Morlet wavelet in both time and frequency domain are shown in Fig. 1(a) and 1(b), respectively.

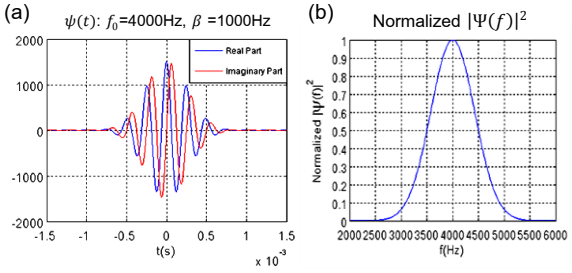

Fig. 1 Morlet wavelet (f_0= 4000Hz, β = 1000Hz) in: (a) time domain (both real and imaginary part), (b) frequency domain

2.2 Envelope analysis

Since bearing defect signal can be viewed as bursts of exponentially decaying sinusoidal vibration at system resonance frequency, i.e. impulse train response of underdamped system. Envelope analysis allows us to extract bearing defect characteristic frequency from the signal using following steps [6]. First, apply bandpass filter to the signal $x(t)$ in Fig. 2(a) around the natural frequency of the system shown in Fig. 2(b) using Eq. (8), to obtain the filtered signal $x_f(t)$ (real part) shown in Fig. 2(c). After that, envelope is applied to the filtered signal as in Fig. 2(e). Since filtered signal obtained from Eq. (8) is analytical signal, therefore modulus of this signal provides the envelope $S(t)$ of the filtered signal [9]:

$$S(t) = \sqrt{\left[Re\left(WT(f_0,\beta)\right)\right]^2 + \left[Im\left(WT(f_0,\beta)\right)\right]^2} \qquad (9)$$

At this point, it is seen that Fig 2(e) is an envelope outline of Fig. 2(c). This allows impulse-related low frequency part to be demodulated from natural-frequency-related high frequency part. Lastly, Fourier spectrum $S(f)$ of $S(t)$ is obtained. If bearing defect occurs, it can be noticed by distinct peaks at defect characteristic frequency and its harmonics as in Fig. 2(f). Note that Fig. 2(b) and 2(d) are Fourier spectrum of Fig. 2(a) and 2(c), respectively.

3. Review on signal modeling of rolling bearing element bearing with localized defect

Impulse is generated when mating contact surface runs pass the defect. Impulse causes wideband excitation to the bearing-support structure, resulting in rise of the natural frequencies peak in the spectrum. In case that transmission path of vibration between location that impulse is generated and location of accelerometer remains the same (defect occur on bearing outer race), the vibration signal $x(t)$ can be modelled as follow [12]:

$$x(t) = \sum_{k=0}^{\infty} A_k h(t - kT_r) + n(t) \qquad (10)$$

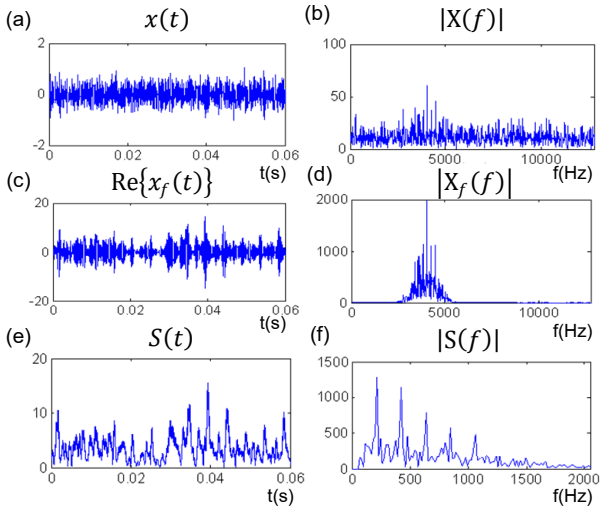

Fig. 2 Envelope analysis: (a) signal $x(t)$, (b) spectrum $|X(f)|$, (c) filtered signal $\mathrm{Re}\{x_f(t)\}$ using Morlet wavelet in Fig 1, (d) spectrum $|X_f(f)|$, (e) envelope $S(t)$ and (f) envelope spectrum $|S(f)|$

Where A_k is the k^{th} defect impulse intensity, $n(t)$ is noise and $h(t - kT_r)$ is impulse response function that has period of excitation T_r corresponding to defect characteristic frequency. The impulse response of a linear underdamped second order system which can be described as:

$$h(t) = \frac{1}{m\omega_d} e^{-\left(\frac{\xi\omega_d}{\sqrt{1-\xi^2}}\right)t} sin\omega_d t \qquad (11)$$

Where m is mass of the system, ξ is damping ratio and ω_d is damped natural frequency of bearing and support structure. Fig. 3(a) and 3(b) show an example of modelled signal and real outer race defect bearing signal, respectively.

In case of inner race and rolling element defect, effect from transmission path and load zone must be considered. Impulse strength function must be added to Eq. (10). However, the modified equation becomes complicated and some parameters are unknown. Hence, this paper will only use the model from Eq. (10) in the simulation part. Refer to [13] for more detail in inner race and roller defect.

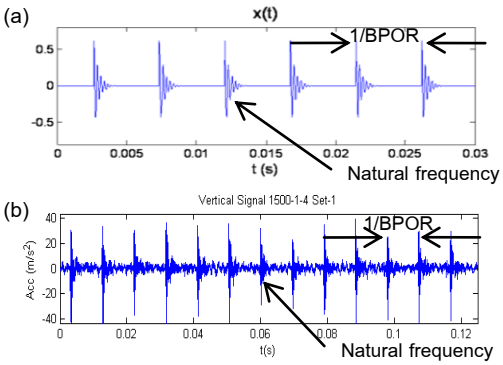

Fig. 3 (a) modelled signal, (b) real outer race defect bearing signal

4. Indicator for Morlet Wavelet Filter Adjustment

In this paper, parameter that takes the distinction of defect characteristic frequency and its harmonics into account is proposed. The key idea of this indicator is to find a set of f_0 and β that gives maximum ratio between the maximum value of sum of peak that falls within the predefined range (from ball spin frequency (BSF) to ball pass inner race frequency (BPIR)) and its harmonics to the arithmetic mean of the envelope spectrum. Hence the higher indicator value, the more distinct of peak and its harmonics in envelope spectrum over the noise floor. Details of procedure are given as below:

(1) Thresholding: threshold is set to be 1 standard deviation above the mean of envelope spectrum

(2) Peak identification: identify all peak of envelope spectrum that exceed threshold. Then find fundamental peaks that have frequencies fall within BSF and BPIR.

(3) Harmonics family identification: classify groups of harmonic family in envelope spectrum. Calculate ratio between sum of

each fundamental peak and its harmonic peaks to the mean defined in (1). The maximum value is used as the indicator of this f_0, β set.

(4) Vary f_0, β throughout the preset f_0, β matrix. Repeat process from (1) to (3) again. A set of f_0 and β that yields maximum indicator is the optimal set.

The overview of steps used to obtain optimal wavelet parameter f_0 and β by using proposed indicator is shown in Fig. 4.

Since process (1) to (4) work along with wavelet transformation and bandpass filtering, some additional constrains must be taken into account

(1) Mother wavelet must have zero mean.

$$\Psi(0) = \int_{-\infty}^{\infty} \psi(t)\, dt = 0 \qquad (12)$$

Actually, Morlet wavelet does not strictly satisfy Eq. (12). However Eq. (12) is very small when f_0/β is large enough, i.e. $f_0/\beta \geq 3.5$ [9]. Hence, this paper states that $f_0/\beta \geq 3.5$

(2) The upper cut-off frequency of Morlet wavelet filter must satisfy sampling theorem

$$f_0 + \frac{\beta}{2} < \frac{f_s}{2} \qquad (13)$$

Where f_s is sampling frequency of the signal.

(3) The lower cut-off frequency should eliminate interfering effects from low frequency vibration.

$$f_0 - \frac{\beta}{2} > N \times f_r \qquad (14)$$

Where f_r is shaft rotational speed and N is positive integer. N is chosen to be 20.

(4) The bandwidth of the filter should be wide enough to cover some sidebands generated by impulse train as shown in spectrum of Fig. 2(a). Hence the bandwidth is chosen as:

$$\beta \geq 500 \text{ Hz} \qquad (15)$$

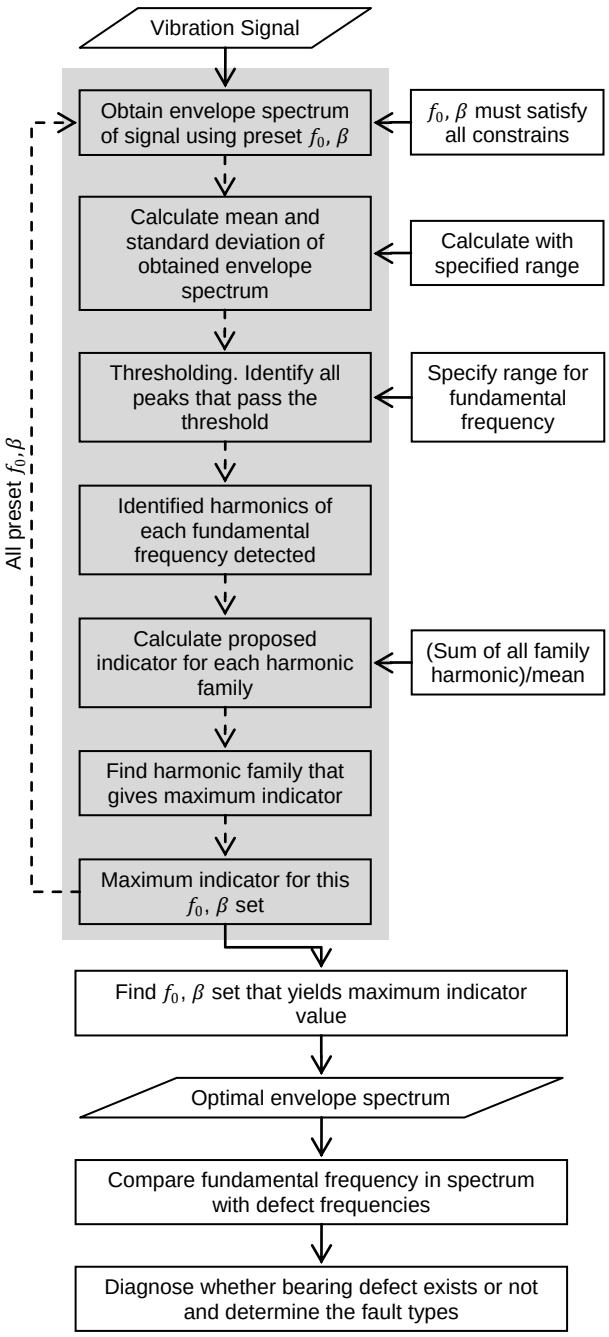

Fig. 4 The overview of steps used to obtain optimal wavelet parameter f_0 and β by using proposed indicator

Fig. 5(a) shows an example of simulated signal and Fig. 5(b) is the corresponding Fourier spectrum of the given signal. Fig. 5(c) shows the contour of the indicator value of the given signal from the matrix of f_0 and β. The optimal set of f_0

and β is shown by the tip of the arrow corresponding to the maximum value of the proposed indicator. Fig. 5(d) is the envelope spectrum of the filtered signal. It clearly shows defect frequency and its harmonics. Note that f_0 of the optimal parameters coincides with the damped natural frequency of the signal as seen in Fig. 5(b)

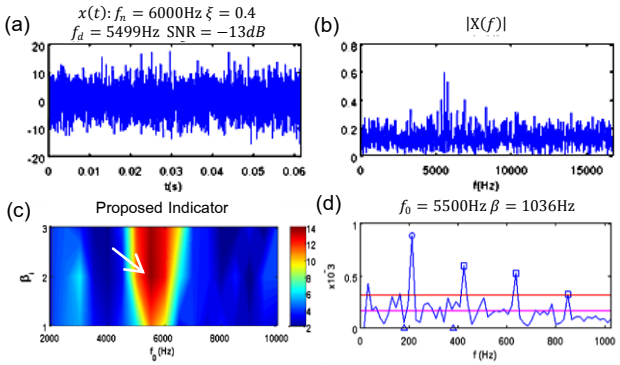

Fig. 5 Example of the envelope spectrum: (a) test signal, (b) spectrum, (c) contour of indicator value for each set of f_0, β and (d) envelope spectrum at optimal indicator

5. Simulation study

In simulation study, simulated defect signal obtained from Eq. (10) and (11) is normalized to make its RMS value equals to 1. Then 100 sets of white noise scaled to the desired signal to noise ratio (SNR) are added to the simulated signal to obtain noisy signals used in the study. After that, sets of f_0, β are used to construct envelope spectrum for the indicator value calculation. All of essential parameters used in simulation study are listed in Table 1.

For each set of the signal at given SNR, there are 100 noisy signals for indicator effectiveness evaluation. The detection result can be categorized into 4 categories which will be mentioned as Cat 1 to Cat 4 in Fig. 6 as stated below:

(1) The optimal envelope spectrum has fundamental frequency of harmonic family that gives maximum indicator value coincides with simulated defect frequency (tolerance is set to be half of envelope spectrum resolution, i.e. 4 Hz). Furthermore, damped natural frequency (f_d) of simulated signal falls within ±250 Hz around f_0. An example is shown in Fig. 5(d)

(2) Almost everything is the same to (1) but f_d falls out of ±250 Hz around f_0.

(3) The optimal envelope spectrum does not have fundamental frequency of harmonic family that gives maximum indicator value coincides with simulated defect frequency. And f_d of simulated signal falls within ±250 Hz around f_0

(4) The optimal envelope spectrum does not have fundamental frequency of harmonic family that gives maximum indicator value coincides with simulated defect frequency. And f_d also falls out of ±250 Hz around f_0.

Table 1 Parameter value in simulation study

Parameter	Value
ξ	0.2, 0.4, 0.6
$f_n = f_d/\left(\sqrt{1-\xi^2}\right)$	4000, 6000, 8000, 10000 Hz
A_k	1
T_r	4.717 ms (corresponds to 212 Hz)
Sampling time	15 μs
Data point	4096
f_0	2000 - 10000 Hz with 500 Hz increment
β	From 1000 Hz to f_0/3.5, 3 equally spaced
SNR	-10, -13, -15 dB

Since the defect frequency is the main interest, the defect is detectable in category 1 and 2 but it is undetectable in category 3 and 4. We will evaluate the effectiveness of the

proposed indicator via these categories. Fig. 6(a) to (c) show effectiveness of proposed indicator in defect detection of signals at various sets of signal undamped natural frequency (f_n) and damping ratio (ξ) at -10, -13 and -15dB SNR. The bar graph is color coded according to each category mentioned earlier. The number of each category that printed on each color bar is the number detected in that category. Note that the number of detectable defect is sum of blue and red color in stacked bar graph.

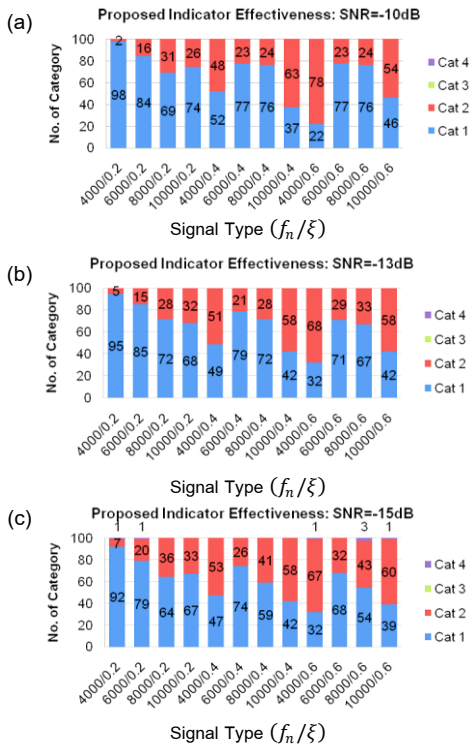

Fig. 6 Effectiveness of proposed indicator of simulation signals in various sets of f_n and ξ at: (a) -10dB, (b) -13dB and (c) -15 dB

It is seen in Fig. 6(a) to (c) that the proposed indicator can detect simulate bearing defect signal with more than 97% accuracy up to SNR =-15dB. The results have high repeatability regardless of signal undamped natural frequency and damping ratio which is preferable for bearing defect detection.

6. Real bearing experiment

Real bearing experiment is performed to validate the model used in simulation study under various speeds (900, 1500, 2100 and 2700 rpm), radial loads (102, 830 and 1558N) and defect sizes (nominal 0.11 and 0.17mm width). The radial load is calculated from loading spring deflection and geometry of loading mechanism) using test rig shown in Fig. 7. The defects are seeded on the outer race of SKF N305 ECP roller bearings (BPOR=4.25xrpm) in the entire bearing width using wirecut as shown in Fig. 8. Note that estimated basic rating life (L_{10h}) of the toughest condition (2700 rpm, 1558N) is 465,900 hours. However, the entire data collection process takes approximately 1.5 hour, so it can be assumed that defect width is not increased. By using microscope, it is confirmed that defect width is not increased at detectable level during the experiment. Fig 9(a) and (b) shows an example of defect before and after the experiment using 50X digital microscope, respectively. Note that there is no noticeable difference in defect size between those two figures.

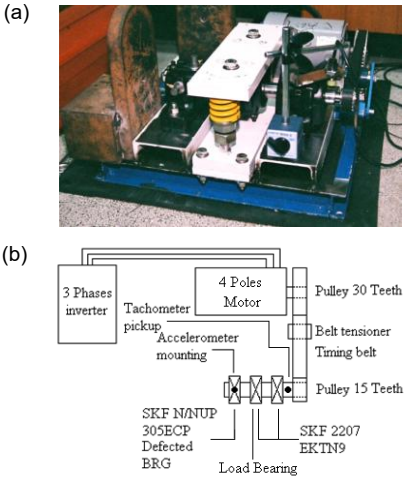

Fig. 7 Bearing test rig (a) test rig (b) schematic diagram

Fig. 8 Overview of defect on the outer race

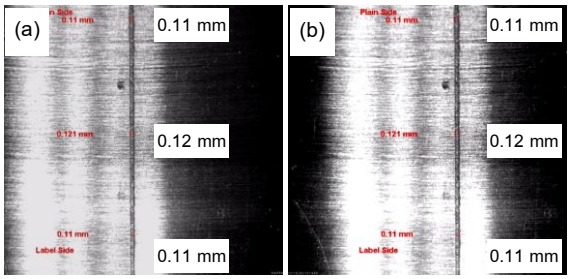

Fig. 9 Example of defect of 0.11mm nominal width (a) before and (b) after the experiment

Signals are sampled at 33kHz sampling frequency and 4096 sampling data per set and 40 sets of measured signal from both vertical and horizontal direction are used in evaluation. Sample spectrums of the signal are shown in Fig. 10(a) and 10(b). Note that BPOR does not exist at low frequency spectrum.

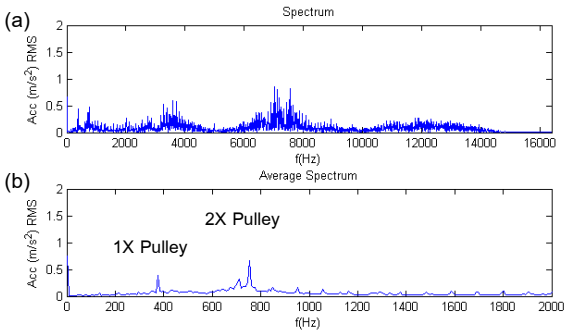

Fig. 10 Defective bearing spectrum at 1500 rpm (BPOR=106.3Hz): (a) spectrum of 1 of 40 set and (b) low frequency average spectrum

The signals are processed using the scheme mentioned in section 4 and the detection result criteria similar to section 5 except only that, in real case, category number is reduce to 2 (detected or undetected) because natural frequency is not concerned. The result are shown in Fig. 11

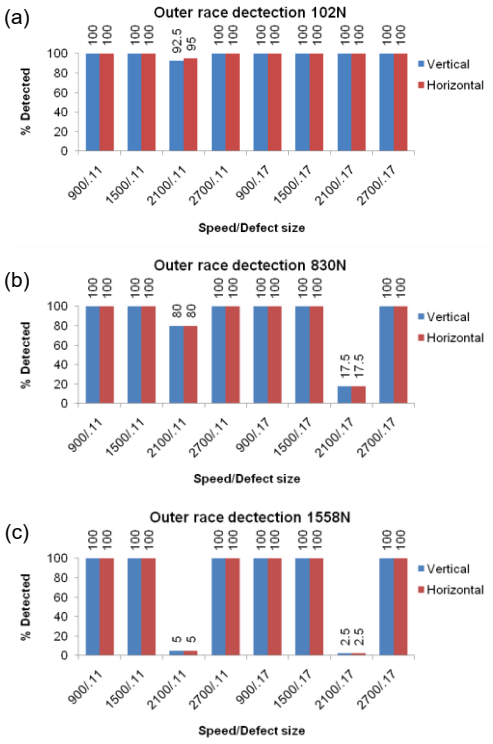

Fig. 11 Detection result (a) 102N, (b) 830N and (c).1558N

From Fig. 11, it is seen that the proposed indicator and detection scheme can detect the defect in majority. However, at speed of 2100 rpm, the defect cannot be detected. This is because BPOR at this speed is in the middle between adjacent lines in envelope spectrum, leading to erroneous result. This problem can be solved by double the sampling data then the resolution of the spectrum line is finer. BPOR can be detected without ambiguousness. The detection result after modification is shown in Fig. 12. It is seen that the modification gives successful detection result.

7. Conclusion

In this paper, an indicator for optimal Morlet wavelet filter has been proposed. Based on the fact that envelope spectrum of periodic

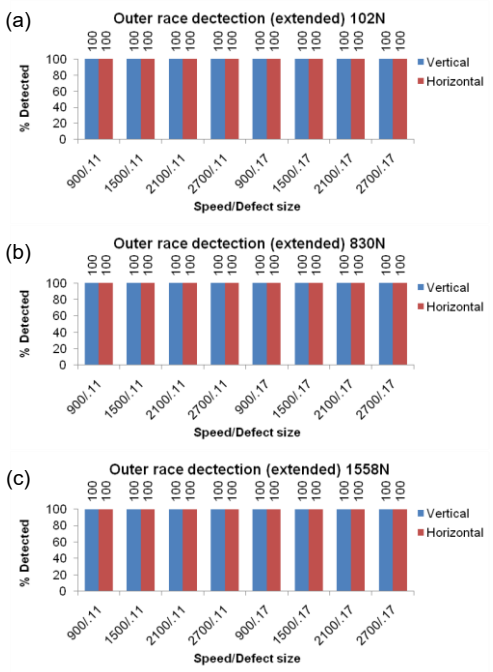

Fig. 12 Detection result (after modification)
(a) 102N, (b) 830N and (c).1558N

impulse response function has harmonics of its excitation frequency. This indicator is the ratio of maximum value of sum of harmonic families that pass the threshold to the arithmetic mean of envelope spectrum in a predefined range. It is used to adjust Morlet wavelet center frequency (f_0) and bandwidth (β). The optimal wavelet is the wavelet that yields maximum value of the indicator.

The proposed indicator is used to analyze the simulated defect signals of various damped natural frequency and damping ratio. It is shown that the proposed indicator achieves more than 97% defect detection accuracy up to SNR =-15dB regardless of signal damped natural frequency and damping ratio.

Lastly, real bearing experiment of outer race defect is performed. Analysis of bearing signal is shown that line resolution in envelope spectrum affects correctness of detection result. Hence, proper resolution should be selected to avoid the case that bearing frequency falls in the middle between two adjacent spectrum lines. In case of proper line resolution, the proposed indicator and detection scheme can detect the outer race defect correctly.

8. Acknowledgement

The research was funded by the Graduate School, Chulalongkorn University.

9. Reference

[1] McFadden, P. D. and Smith, J. D., Vibration monitoring of rolling element bearings by the high frequency resonance technique - A review, *Tribology International*, Vol. 17, pp. 1-18, 1984.

[2] Li, C. J. and Ma, J., Wavelet decomposition of vibrations for detection of bearing-localized defects, *NDT&E International*, Vol. 30, No. 3, pp. 143-149, 1997.

[3] Nikolaou, N. G. and Antoniadis, I. A., Demodulation of vibration signals generated by defects in rolling element bearings using complex shifted Morlet wavelet, *Mechanical System and Signal Processing*, Vol. 16, No. 4, pp. 677-694, 2002.

[4] Yiakopoulos, C. T. and Antoniadis, I. A., Wavelet based demodulation of vibration signals generated by defects in rolling element bearings, *Shock and Vibration*, Vol. 9, pp. 293-306, 2002.

[5] Qiu, H., Lee, J., Lin, J. and Yu, G., Wavelet filter-based weak signature detection method and its application on rolling element bearing prognostics, *Journal of Sound and Vibration*, Vol. 289, pp. 1066-1090, 2006.

[6] Shiroishi, J., Li, Y., Liang, S., Danyluk, S. and Kurfess, T., Vibration analysis for bearing outer race condition diagnostics, *Journal of the Brazilian Society of Mechanical Sciences*,

Vol. 21, No. 3, 1999.

[7] Sheen, Y. T., On the study of applying Morlet wavelet to the Hilbert transform for the envelope detection of bearing vibrations, *Mechanical System and Signal Processing*, Vol. 23, pp. 1518-1527, 2009.

[8] Su, W., Wang, F., Zhu, H., Zhang, Z. and Guo, Z., Rolling element bearing faults diagnosis based on optimal Morlet wavelet filter and autocorrelation enhancement, *Mechanical System and Signal Processing*, Vol. 24, pp. 1458-1472, 2010

[9] He, W., Jiang, Z. N., Feng, K., Bearing fault detection based on optimal wavelet filter and sparse code shrinkage, *Measurement*, 2009.

[10] Addison, P. S., The Illustrated *Wavelet Transform Handbook: Introductory Theory and Applications in Science, Engineering, Medicine and Finance*, Taylor and Francis, New York, 2002.

[11] Yang, W. and Ren, X., Detecting impulses in mechanical signals by wavelets, *EURASIP Journal of Applied Signal Processing*, pp. 1156-1162, 2004.

[12] Junsheng, C., Dejie Y. and Yu, Y., Application of an impulse response wavelet to fault diagnosis of rolling bearing, *Mechanical System and Signal Processing*, Vol. 21, pp. 920-929, 2007.

[13] Harris, T.A., *Rolling Bearing Analysis*, 4th Edition, Wiley, New York, 2001.